Science Advances
AAAS

advances.sciencemag.org/cgi/content/full/7/28/eabf0851/DC1

Supplementary Materials for

Revealing the source of Jupiter's x-ray auroral flares

Zhonghua Yao*, William R. Dunn, Emma E. Woodfield, George Clark, Barry H. Mauk, Robert W. Ebert, Denis Grodent, Bertrand Bonfond, Dongxiao Pan, I. Jonathan Rae, Binbin Ni, Ruilong Guo, Graziella Branduardi-Raymont, Affelia D. Wibisono, Pedro Rodriguez, Stavros Kotsiaros, Jan-Uwe Ness, Frederic Allegrini, William S. Kurth, G. Randall Gladstone, Ralph Kraft, Ali H. Sulaiman, Harry Manners, Ravindra T. Desai, Scott J. Bolton

*Corresponding author. Email: z.yao@ucl.ac.uk

Published 9 July 2021, *Sci. Adv.* **7**, eabf0851 (2021)
DOI: 10.1126/sciadv.abf0851

This PDF file includes:

Supplementary Text

Demonstration of the coordination between Earth orbit space telescope and Juno's in situ measurements in dawnside magnetodisc.

As indicated by Fig. S2(A) and S2(B), planetary rotation drives plasmadisc oscillation (vertically) and lead to periodical enhancements of proton and electron fluxes when Juno entered into the plasma sheet. Figure S2(C) shows CML indicating which part of the planet (i.e., longitude range) is facing Earth during an observation (e.g., Fig. S1). Usually an Earth orbit telescope (e.g., XMM, Hubble Space Telescope etc.) could well capture the polar auroral region where X-ray emissions are believed to originate from when CML ranges from 110 to 210 degrees (the red colored lines). From the comparison between Fig. S2(A), S2(B) and S2(C), we could find that when Juno was measuring plasma sheet, an Earth orbit telescope could provide good simultaneous observing windows for the polar X-ray source region. Figure S2(D) shows magnetic field B_r and distance between Juno and the magnetic equator. Juno continually approached to the plasma sheet after the north magnetic pole tilted to the spacecraft's local time at ~4.5 MLT (i.e., the minimum distance between Juno and the magnetic equator), and eventually entered plasma sheet at 1-3 hours later as evidenced by the rapid changes of magnetic field and electron flux enhancements. The time delay between Jupiter's magnetic equator oscillation and plasma sheet oscillation provides an ideal chance for simultaneous in situ measurements in the plasma sheet and remote sensing of aurora at Earth orbit.

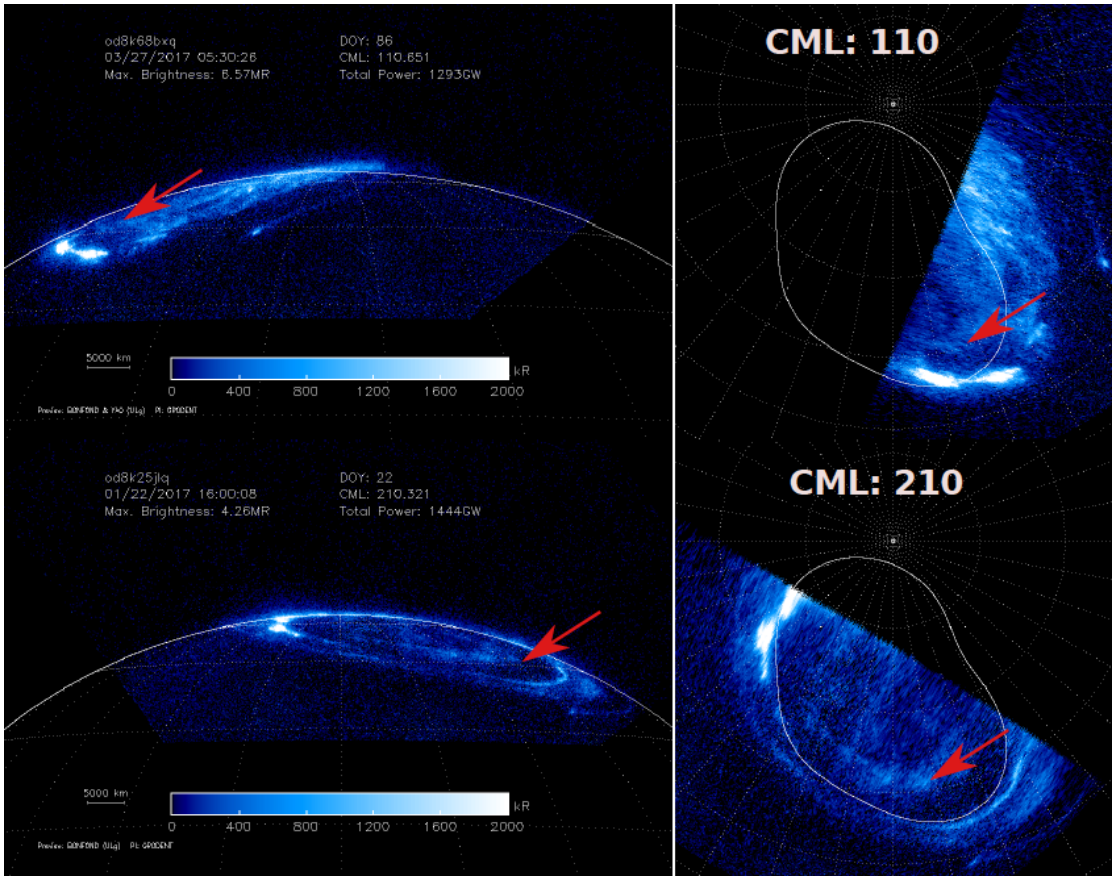

Fig. S1. Two auroral examples showing the viewing geometry when CML at 110 and 210 degrees.

The two auroral images were obtained from the Hubble Space Telescope. The left images are the view from Earth orbit, and the right images are polar projections fixed in Jupiter. As indicated by the red arrows, X-ray emissions are believed to originate from the polar region of the main auroral oval (*1*). This region comes to the field of view of a telescope in Earth orbit when the CML is at ~110 degrees, and the polar auroral region leaves the telescope's field of view when the CML is at ~ 210 degrees. The two images were from HST program to support Juno mission (proposal ID: 14634, PI: Denis Grodent).

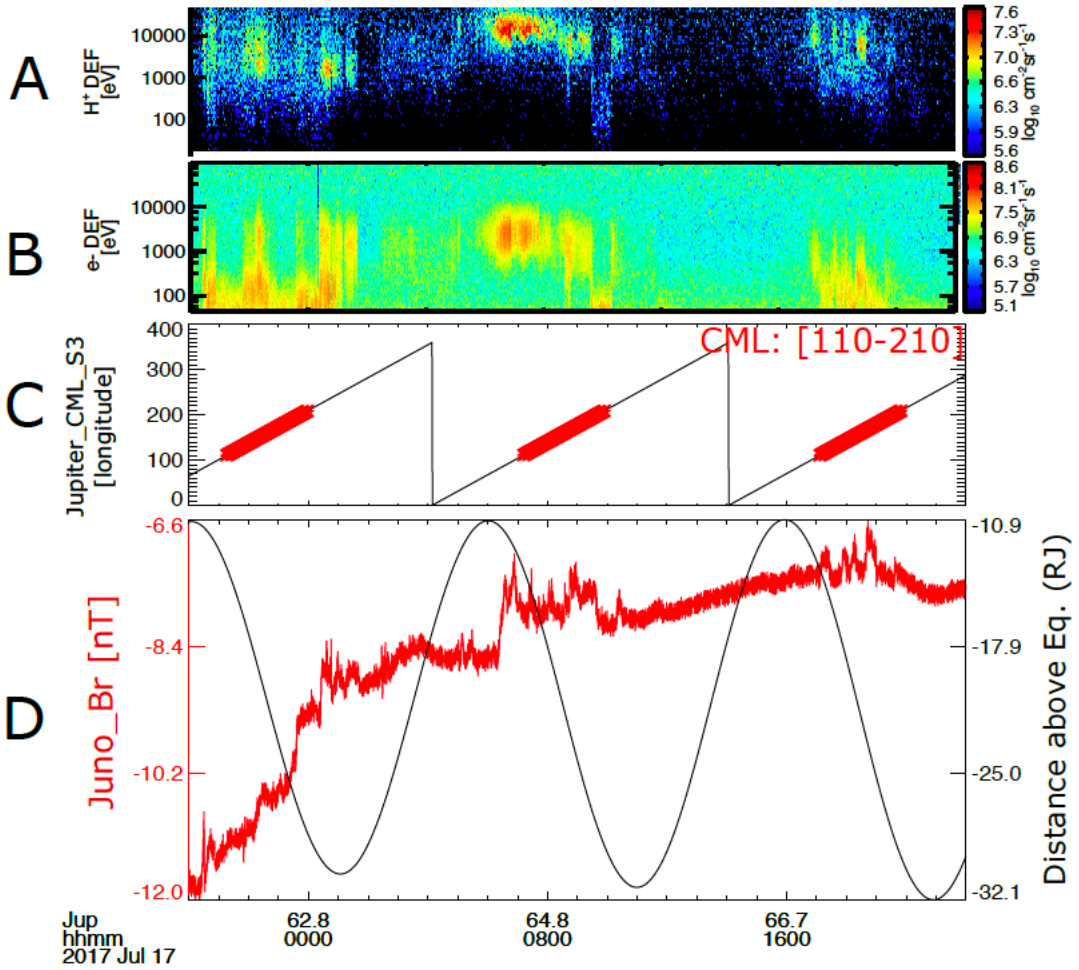

Fig. S2. Demonstration of the modulation caused by planetary rotation.

Intensity versus energy distributions for protons (A) and electrons (B) measured by Juno-JADE between July 16th 20 UT and July 17th 22 UT. c, System III central meridian longitude (CML). The red colored line in Fig. S2(C) highlights CML between 110 and 210 degrees, when the northern polar aurora could be well captured by the telescope from the Earth orbit. Two examples are given in Fig. S2(D), the red curve shows the magnetic component Br in System III coordinate system, and the black curve shows the distance between Juno and Jupiter's magnetic equator.

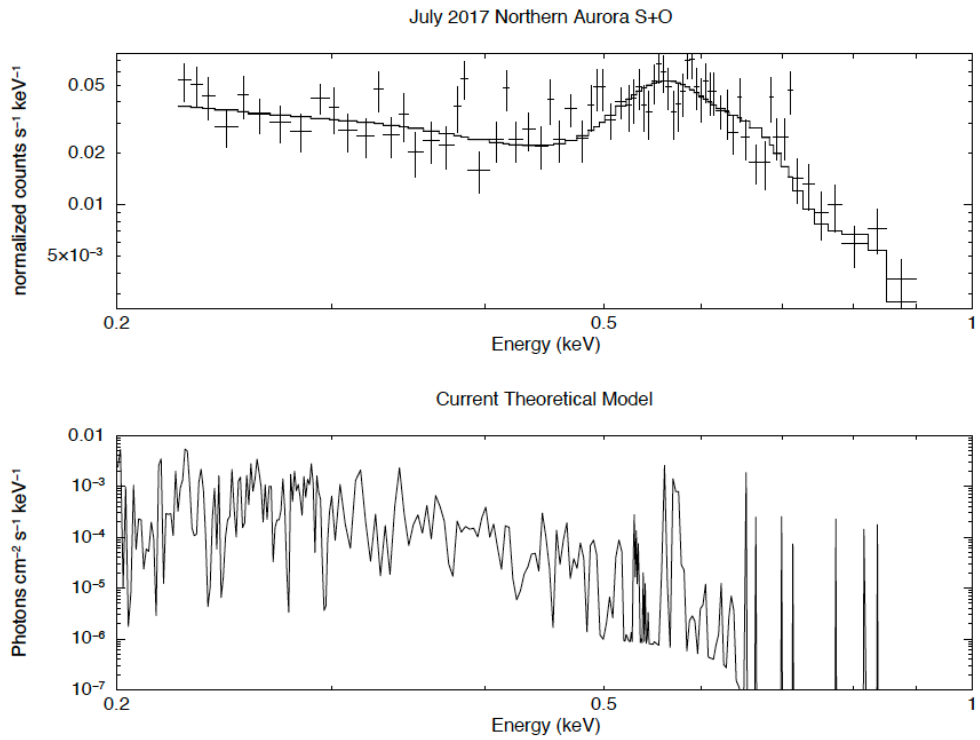

Fig. S3. Model fitting of X-ray spectrum.

The top panel shows Jupiter's Northern aurora X-ray spectrum as observed by XMM-Newton's EPIC-pn instrument on July 16-17 2017 (black crosses). This spectrum has been fit with an atomic charge exchange model (*33-34*) for sulphur and oxygen ions, which provided a nice fit ($\boldsymbol{\chi^2 \sim 1}$) to the data, evidencing its production by the atmospheric precipitation of sulphur and oxygen ions during this window. The bottom panel shows this theoretical spectrum of charge exchange lines from sulphur and oxygen. The model is convolved with the instrument response to produce the black line overlaid on the data in the top panel.

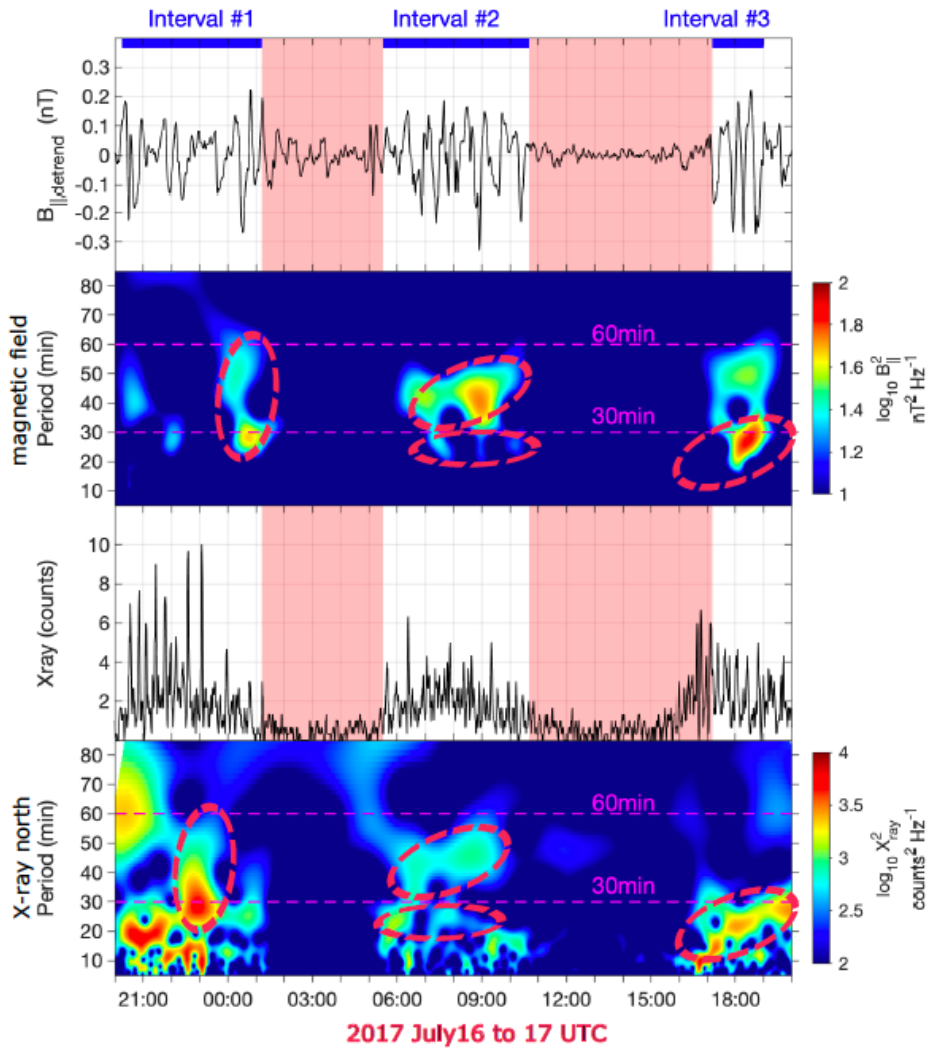

Fig. S4. Wavelet results of the magnetic field and X-ray emission.

Detrended field-aligned magnetic field component (the top panel) and X-ray emission (the third panel) from the northern pole of Jupiter, at a time resolution of one minute. The second and fourth panels are wavelet power spectra of the two variables. During two intervals marked by the light red shadows, the northern pole had rotated to the night side of the planet and therefore wasn't observable by XMM. Due to the spacecraft location and Jupiter's rotation, Juno was in a lobe region during these intervals so that EMIC waves were not observable. In order to reduce the spacecraft's trajectory modulation due to the large-scale plasma sheet oscillation, we detrended the field-aligned magnetic component $\mathbf{B}_{\|}$ with magnetic field averaged over 40 minutes as the baseline. During the three intervals of enhanced X-ray emissions (also compressional magnetic perturbations), the wave power spectrum shows multiple periodicities from ~10 minutes to 60 minutes.

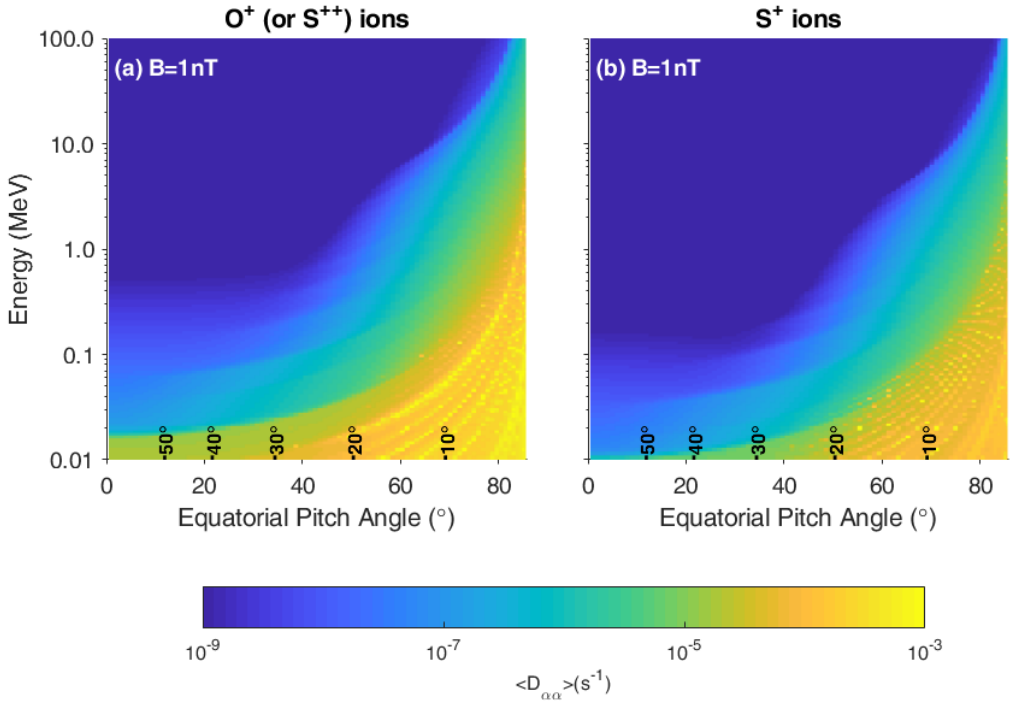

Fig. S5. Local Pitch angle diffusion coefficients Dαα.

The Local Pitch angle diffusion coefficients is calculated using the PADIE code (*45*) from a combination of H+, O+ (S++) and S+ waves calculated locally at B ~ 1 nT interacting with O+ (S++) and S+ ions